

# Cross-Plane Seebeck Coefficient Anomaly in a High Barrier Superlattice with Miniband Formation

Daryoosh Vashaee<sup>1</sup>, Yan Zhang<sup>1</sup>, Gehong Zeng<sup>2</sup>, Yi-Jen Chiu<sup>2</sup>, and Ali Shakouri<sup>1</sup>

<sup>1</sup>Electrical Engineering Dept. University of California, Santa Cruz, CA 95064, USA

<sup>2</sup>Electrical and Computer Engineering Dept., Univ. of California, Santa Barbara, CA 93106

## ABSTRACT

We have measured the cross-plane Seebeck coefficient of short period InGaAs/InAlAs superlattices with 5nm wells and 3nm barriers with different doping concentrations. Contrary to the behavior of conventional bulk III-V materials, the Seebeck coefficient did not decrease monotonically with increasing doping concentration. A detailed numerical calculation based on semi-classical Boltzmann transport equation was developed that takes into account miniband formation. This model can explain the thermopower anomaly that was measured for superlattices with doping concentrations varying from  $2 \times 10^{18}$  to  $3 \times 10^{19}$  cm<sup>-3</sup>. Based on this model, we proposed a structure for an n-type material with a positive Seebeck coefficient. N-type semiconductors normally have a negative Seebeck coefficient. It is shown that in a suitable superlattice structure it is possible to selectively emit “low” energy electrons from the anode to the cathode. Thus, the heat transferred from the anode to the cathode is equivalent to a material with a positive Seebeck coefficient. This will be useful in cascading thermoelements because changing the doping material during the growth is not necessary.

## INTRODUCTION

Thermionic emission cooling in heterostructures has been proposed by Shakouri *et al.*<sup>1</sup> to overcome the limitations of vacuum thermionics at lower temperatures<sup>2</sup>. In the linear transport regime, thick barrier InGaAs/InAlAs superlattices have been predicted to provide close to an order of magnitude improvement in the overall  $ZT$  over the bulk InGaAs value.<sup>3</sup> In this paper we will examine the experimental and theoretical thermoelectric properties of short period InGaAs/InAlAs superlattices. Contrary to the structures studied in reference [3], miniband transport is essential in the calculation of the thermoelectric properties of the superlattice structures introduced in this paper.

## EXPERIMENTS

N-type InGaAs/InAlAs multilayers lattice-matched to InP substrate were grown using molecular beam epitaxy (MBE). Each device consists of a superlattice and 0.5 $\mu$ m-thick highly doped ( $1 \times 10^{19}$  cm<sup>-3</sup>) InGaAs layers used as the top and bottom contact regions. The superlattice contained 25 periods of 5nm thick n-doped InGaAs with varying silicon doping concentrations,  $2 \times 10^{18}$ ,  $4 \times 10^{18}$ ,  $8 \times 10^{18}$  to  $3 \times 10^{19}$  cm<sup>-3</sup>, and 3nm thick undoped InAlAs. Devices with various sizes (70-100 microns in diameter) were fabricated using conventional lithography, dry etching, and metallization techniques. Ni/AuGe/Ni/Au was used to make ohmic contacts to both

electrodes. A thin film heater was deposited on top of the microcooler and used as both a heat source and temperature sensor. At last, the sample was attached to a package, wire bonded, and loaded into the cryostat for measurements. There were total of four samples under test with different doping concentrations. We used two device sizes,  $100 \times 100 \mu\text{m}^2$  and  $70 \times 70 \mu\text{m}^2$  for measurements. First, we calibrated the heater resistance with the stage temperature. To reduce the influence of the contact wires and pads, we used a four-wire measurement for gauging the resistance. At a given heater power, the top of the superlattice device was heated up by the thin film heater to a fixed temperature ( $T_h$ ). The substrate was attached to the heatsink inside the cryostat, where the temperature was controlled by the flow of liquid Helium ( $T_s$ ). The temperature difference across the device ( $\Delta T = T_h - T_s$ ) generates a voltage difference ( $\Delta V$ ), which can be measured by probing the microcooler and ground contacts. Thus, the effective Seebeck coefficient of the device could be calculated easily from  $S = \Delta V / \Delta T$ . The  $\Delta V$  and  $\Delta T$  are the voltage and temperature differences across the device. As long as we could measure the voltage and temperature differences accurately, the Seebeck coefficient could be calculated. The difficulty of characterizing the Seebeck coefficient of a superlattice thin film lies in simultaneously measuring the voltage and temperature drops to within a few microns on both sides of a thin film<sup>4,5</sup>. The Seebeck coefficients were measured at cryostat temperature changes from 50K to 300K. Figure 1 illustrates the measured Seebeck coefficients for samples A, B, C, D with doping concentrations ranging from  $2 \times 10^{18}$  up to  $3 \times 10^{19}$  cm<sup>-3</sup>. From the graph, we can see the Seebeck coefficient increases with temperature from 10K to 300K for all samples. The Seebeck coefficients measured using  $100 \times 100 \mu\text{m}^2$  (squares) and  $70 \times 70 \mu\text{m}^2$  (circles) devices match very well, except for one case (sample D). We found that the discrepancy was due to a heater fabrication error for the  $100 \times 100 \mu\text{m}^2$  sample D.

## THEORETICAL ANALYSIS

For the calculation of the transport coefficients of these samples, we use the model presented in reference [3] with some changes in the key equations for our purpose here. In brief, a linear Boltzmann transport equation was used to calculate the thermoelectric characteristics of the InGaAs bulk device. As for the superlattice properties, since the barrier layer thickness is short and the miniband transport is dominant, the transmission probability is calculated using the Transfer Matrix Method (TMM). The resulting minibands' widths are either on the order

of, or larger than the thermal energy ( $\sim 20\text{meV}$  and  $100\text{meV}$  for the first two minibands). Thus, a bulk-type Boltzmann transport with a correction due to the quantum mechanical transmission

$$n_e(V) = \frac{1}{4\pi^3} \left[ \frac{L_w}{L_p} \int_{-\infty}^{\infty} dk_z \frac{\hbar^2 k_z^2}{m_w^*} \int_{-\infty}^{\infty} dk_x \int_{-\infty}^{\infty} dk_y \left( -\frac{\partial f(k_x, k_y, k_z, E_f)}{\partial E} \right) T(k_z, V) \right. \\ \left. + \frac{L_b}{L_p} \int_{-\infty}^{\infty} dk_z \frac{\hbar^2 k_z^2}{m_b^*} \int_{-\infty}^{\infty} dk_x \int_{-\infty}^{\infty} dk_y \left( -\frac{\partial f(k_x, k_y, k_z, E_f - E_b)}{\partial E} \right) T(\sqrt{k_z^2 + k_b^2}, V) \right] \quad (1)$$

where  $V$  is the applied voltage;  $L_w$  ( $L_b$ ) is well (barrier) thickness,  $L_p=L_b+L_w$ ;  $k_x, k_y, k_z$ , are the components of electron momentum;  $E_f$  is the Fermi energy;  $f$  is the Fermi-Dirac distribution function. The transmission probability  $T$  depends only on the  $V$  and  $k_{z_i}$  values since we have assumed that the lateral momentum is conserved. The first and second integrals are the number of moving electrons at the well and barrier regions respectively. Electrical conductivity, Seebeck coefficient, and the effective thermoelectric figure-of-merit

above and below the barrier is assumed. This is shown in equation 1 for the number of electrons participating in the superlattice transport:

( $ZT$ ) can be calculated as stated in reference [3]. Parameters used in the calculations are listed in table I. <sup>6</sup> Theoretical calculations are presented for well and barrier widths of 52 and  $25\text{\AA}$ , respectively, which gave a better fit to experimental results. The thickness deviation compared to the nominal values was verified with the use of X-Ray diffraction that showed a superlattice period of  $77\text{\AA}$ .

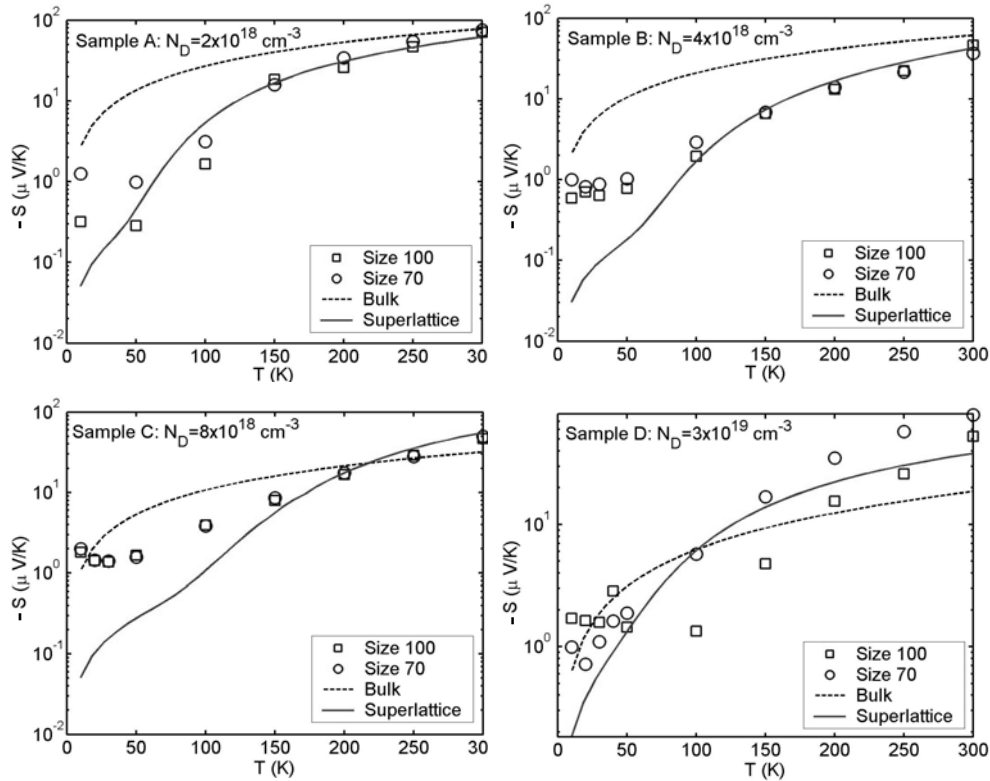


**Figure 1:** The measured Seebeck coefficient for Samples A, B, C, D. Squares (device size  $100 \times 100 \mu\text{m}^2$ ) and circles (device size  $70 \times 70 \mu\text{m}^2$ ) are experimental data, the lines are theoretical modeling.

**Table I:** Structural parameters for the  $\text{In}_{0.53}\text{Ga}_{0.47}\text{As}/\text{In}_{0.52}\text{Al}_{0.48}\text{As}$  superlattice

$n_w$	$L_w$ (nm)	$L_b$ (nm)	$V_b$ (meV)	$m_w^*$	$m_b^*$	$\alpha_w$ ( $\text{eV}^{-1}$ )	$\alpha_b$ ( $\text{eV}^{-1}$ )	$\mu_w$ ( $\text{cm}^2/\text{Vs}$ )	$\mu_b$ ( $\text{cm}^2/\text{Vs}$ )	$v_s$ ( $\text{cm/s}$ )
250	50	30	520	0.045 <sup>7</sup>	0.073	1.45 <sup>8</sup>	1.45	1000	6000	10 <sup>7</sup>

Theoretical modeling shows that the Seebeck coefficient monotonically decreases with doping concentrations up to  $10^{19}$   $\text{cm}^{-3}$ , but it starts to increase as the doping concentration is further increased. This trend was confirmed by the increased Seebeck coefficient measured for Sample D. The calculated Seebeck coefficients for samples A to D are shown in Figure 1. As it can be seen in this figure, sample D's Seebeck coefficient is larger than that of bulk InGaAs doped at the same level when  $T > 100\text{K}$ , while the Seebeck coefficients of samples A and B were lower than bulk values over the whole temperature range. Theoretical calculations and experimental results match very well at low doping concentrations over the whole temperature range (Fig.1, sample A). However, as doping increases the theory underestimates the measured low temperature Seebeck coefficient. We are currently investigating corrections due to package thermal resistance and substrate Seebeck coefficient in order to explain the low temperature Seebeck results ( $T < 100\text{K}$ ). However, it is clear from both theory and experiment that at temperatures higher than 100-150K, Seebeck coefficient does not have a monotonic dependence with doping and the Seebeck coefficient of sample D ( $2-3 \times 10^{19}$   $\text{cm}^{-3}$ ) is larger than lower doped samples.

## DISCUSSIONS

In a qualitative picture, the Seebeck coefficient is the average energy transported by the charge carriers corresponding to a diffusion thermopower. In a superlattice if the miniband is wide enough in energy and the Fermi energy is placed approximately  $k_B T$  above the miniband, it is possible to selectively block electrons above the Fermi level, and transmit electrons below the Fermi energy. Consequently, heating and cooling would be reversed. The barrier energy must be also far enough away from the miniband to effectively block higher energy electrons from passing over the barrier. This can explain the thermopower anomaly seen in Figure 1. Because many of the high energy electrons above the Fermi level are blocked as the Fermi level approaches the first miniband, the thermopower is reduced (doping increase in samples A, B and C). However, when the Fermi level increases significantly above the miniband (sample D), many of the low energy electrons below the Fermi level are blocked, thus the thermopower increases.

Cantrell et al.<sup>9</sup> and Larsson et al.<sup>10</sup> have predicted that in a suitable multiple barrier structure, the thermopower may change sign because of a quantum transport process. However, they were not concerned with the thermoelectric figure-of-merit (ZT). Theoretical modeling in both of the above references is different from what is presented in this paper. Hence, their analysis ends up with somehow different results. For example, contrary to the results of reference [10], the sign of the Seebeck coefficient does not change for any value of a doping concentration. This is shown in Figure 2 where the Seebeck coefficient and the effective thermoelectric figure-of-merit are calculated for the

structure shown in table I. One may expect that the sign of the Seebeck coefficient changes according to the description in the beginning of this section. However, we see that the sign does not change, but the Seebeck coefficient reduces significantly to about 25  $\mu\text{V/K}$ . This reduction in the Seebeck coefficient happens when the Fermi energy approaches the second miniband as well. This is due to two key assumptions made in reference<sup>10</sup>: (1) Electron transport in superlattice minibands is in the non-linear regime (2) The transmission probability depends on electron's kinetic energy in cross-plane, which implies the lateral momentum of electrons is conserved. The former assumption is only true for electron transport in *narrow* minibands. However, superlattice minibands in samples A-D are too *wide* to yield such a thermopower anomaly. In consequence, their formalism is not able to explain the measured experimental data presented in this paper. For applications where the superlattice miniband is wide, non-linear transport equations must be replaced with a better approximation based on linear transport theory. Our approach in this paper is based on the latter assumption and thus can explain the experimental results.<sup>3</sup> Although there is still the thermopower anomaly seen in Figure 2-left for the conserved lateral momentum case, the sign of the Seebeck coefficient does not change. It is shown in Figure 2 that the sign change in Seebeck coefficient at the given temperature happens only if the lateral momentum of electrons is not conserved.<sup>3,11,12</sup>

In N-type semiconductors, the Seebeck coefficient is negative while P-type materials generally have positive Seebeck coefficient. Figure 2 proposes a superlattice structure that can provide positive Seebeck coefficient in N-type materials when the lateral momentum is not conserved. This will be very useful in cascading thermoelements because changing the doping material during the growth will no longer be necessary. However, the ZT for superlattice structures in miniband conduction regime is generally smaller than that of the bulk from the same material. This can discourage the use of superlattice structures in the design of cascade-thermoelectric devices. Nevertheless, it is shown that if the lateral momentum of electrons transported over a superlattice barrier becomes non-conserved by means of introducing scattering centers in the structure, the ZT can be significantly improved.<sup>3,11</sup> This improvement in ZT is also shown in Figure 2: the ZT for the superlattice structure in the non-conserved case is about five times larger than that of bulk value. It should be noted that in order to isolate the thermoelectric performance improvement due to the thermionic emission of electrons over the barrier, we are not considering the reduction in lattice thermal conductivity in our comparison of bulk and superlattice structures (all have a thermal conductivity of 5W/mK at room temperature). Taking thermal conductivity reduction into account would cause an even higher ZT in the superlattices.

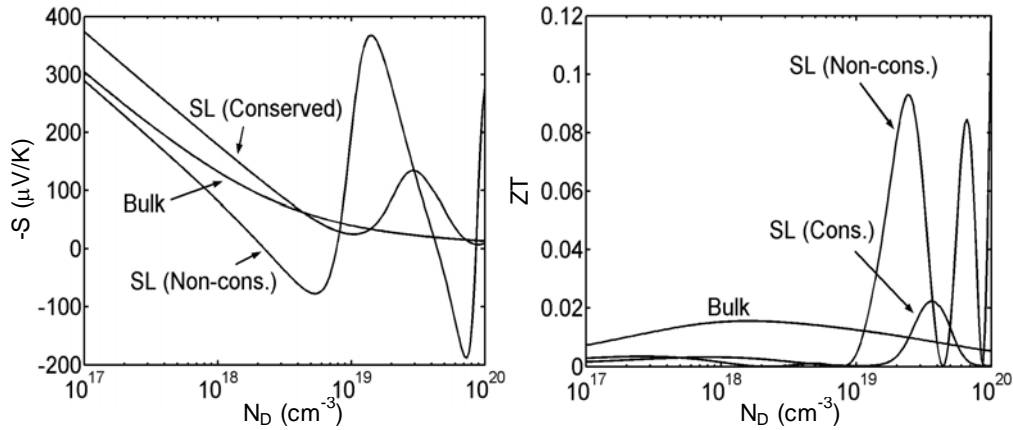


**Figure 2:** The Seebeck coefficient (left) and thermoelectric figure-of-merit (right) vs. doping concentration for InGaAs bulk and InGaAs/InAlAs superlattice for two cases of conserved and non-conserved lateral momentum.

## CONCLUSION

In a superlattice it is possible to form minibands for electron transmission. In cases where energy separation between minibands is several times thermal energy ( $k_B T$ ), electron transport above or below Fermi-energy could be selected. Thus the Seebeck coefficient could be either positive or negative. However, we did not observe the sign change experimentally, as shown in Figure 1. When we carefully examined the theoretical model, we found out that the sign of the Seebeck coefficient could be changed only when the electron's lateral momentum is not conserved during quantum mechanical transmission (see Figure 2). Lateral momentum conservation is a consequence of translational symmetry in the plane of quantum wells and it could be broken using e.g. embedded quantum dots. Calculations in Ref. <sup>13</sup> also illustrate how the Seebeck coefficient sign changes as p-doping increases for Ge/Si quantum dots superlattices. This would make it possible to make *n*- and *p*-type thermoelectric elements with the same doping material. This is very favorable in a configuration of multi thermo elements connected electrically in series and thermally in parallel.

## ACKNOWLEDGEMENT

This work was supported by the MURI TEC Center and the Packard Fellowship.

## REFERENCES:

- <sup>1</sup> A. Shakouri, E.Y. Lee, D.L. Smith, V. Narayanamurti, J.E. Bowers, "Thermoelectric effects in submicron heterostructure barriers," *Microscale Thermophysical Engineering* 2 (37) 1998.
- <sup>2</sup> G.D. Mahan, "Thermionic refrigeration," *Journal of Applied Physics*, Vol. 76, No.7, 1 Oct. 1994, p. 4362-6.
- <sup>3</sup> D.Vashae, and A. Shakouri, "Electronic and Thermoelectric Transport in Semiconductor and Metallic Superlattices", *Journal of Applied Physics*, Volume 95, Issue 3, pp. 1233-1245, February 1, 2004.

- <sup>4</sup> Zhang, Y.; Zeng, G.; Singh, R.; Christofferson, J.; Croke, E.; Bowers, J.E.; Shakouri, A. "Measurement of Seebeck coefficient perpendicular to SiGe superlattice layers," 21st International Conference on Thermoelectrics, Long Beach CA, 26-29 August 2002.
- <sup>5</sup> Chen, G., *Phys. Rev. B*, 57 P14958, 1998.
- <sup>6</sup> Doping concentrations were determined to be  $2 \times 10^{18}$ ,  $3 \times 10^{18}$ ,  $9 \times 10^{18}$ , and  $2.3 \times 10^{19} \text{ cm}^{-3}$  to fit the experimental data of samples A, B, C, and D respectively. For all samples it is assumed that only wells are doped.
- <sup>7</sup> K. Tanaka, N. Kotera, H. Nakamura, "Nonparabolic tendency of electron effective mass estimated by confined states in  $\text{In}_{0.53}\text{Ga}_{0.47}\text{As}/\text{In}_{0.52}\text{Al}_{0.48}\text{As}$  multi-quantum-well structures". *Superlattices and Microstructures*, Vol. 26, No. 1, 1999.
- <sup>8</sup> Pau Garcias-Salvà, Lluís Prat Viñas, "Inclusion of the Conduction Band non-Parabolicity in the Monte Carlo Simulation of Abrupt HBTs".
- <sup>9</sup> D G Cantrell and P N Butcher, *J. Phys. C: Solid State Phys.* **18** (1985) L587-L592.
- <sup>10</sup> Magnus Larsson, Vadim B. Antonyuk, A. G. Mal'shukov, and K. A. Chao, "Thermopower anomaly in multiple barrier structures", *Physical Review B* 68, 233302, 2003.
- <sup>11</sup> D. Vashae, A. Shakouri. *Physical Review Letter*, Vol.92, no. 10, Mar. 2004, pp. 106103-1.
- <sup>12</sup> Daryoosh Vashae and Ali Shakouri, *Mat. Res. Soc. Symp. Proc. (Thermoelectric Materials 2001-Research and Applications)*, Vol. 691, pp.131-145, Boston, MA, Nov. 2001.
- <sup>13</sup> Alexander A. Balandin and Olga L. Lazarenkova, "Mechanism of thermoelectric figure-of-merit enhancement in regimented quantum dot superlattices", *Appl. Phys. Lett.*, Vol. 82, No.3, P415, 2003.